Supplement of Atmos. Meas. Tech., 9, 5555–5574, 2016
http://www.atmos-meas-tech.net/9/5555/2016/
doi:10.5194/amt-9-5555-2016-supplement

Atmospheric Measurement Techniques
Open Access
EGU

Supplement of

Information content and sensitivity of the $3\beta + 2\alpha$ lidar measurement system for aerosol microphysical retrievals

Sharon P. Burton et al.

Correspondence to: Sharon P. Burton (sharon.p.burton@nasa.gov)

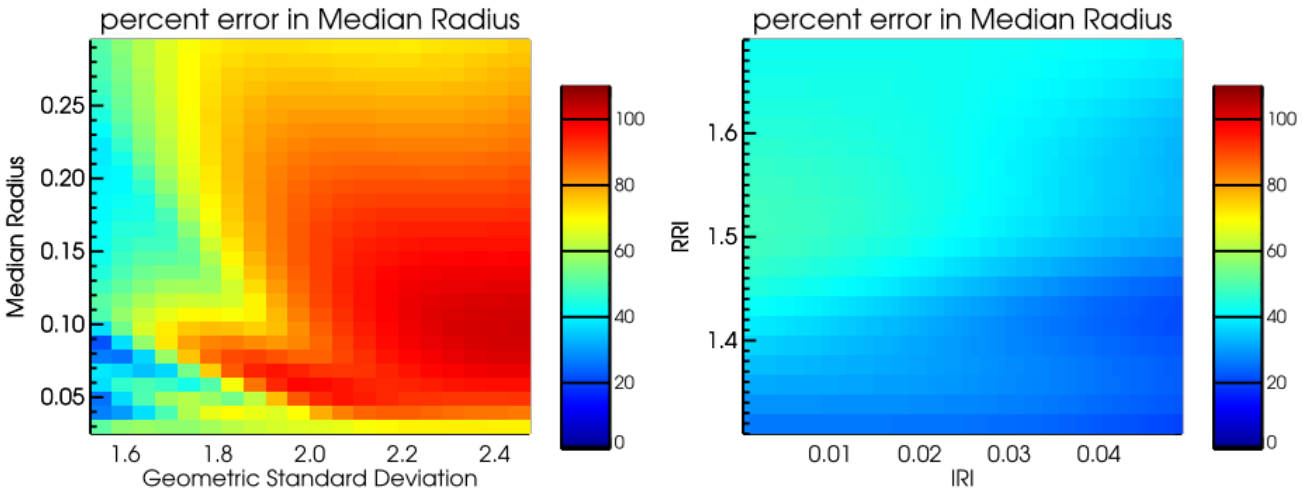

Figure S 1. The a posteriori standard deviation in the median radius is here shown as a percent error, as 2-D slices through the five variable state space. The left figure shows the dependence on median radius and geometric standard deviation, with the complex refractive index held fixed as 1.47-0.00325i and the total number concentration held fixed at 1001 cm^{-3}. The right figure shows the dependence on the complex refractive index (RRI = real refractive index and IRI = imaginary refractive index) with the total number concentration held fixed at 1001 cm^{-3}, the median radius = 0.115 µm, and the geometric standard deviation = 1.475. Dependence on total number concentration is slight and is not illustrated here.

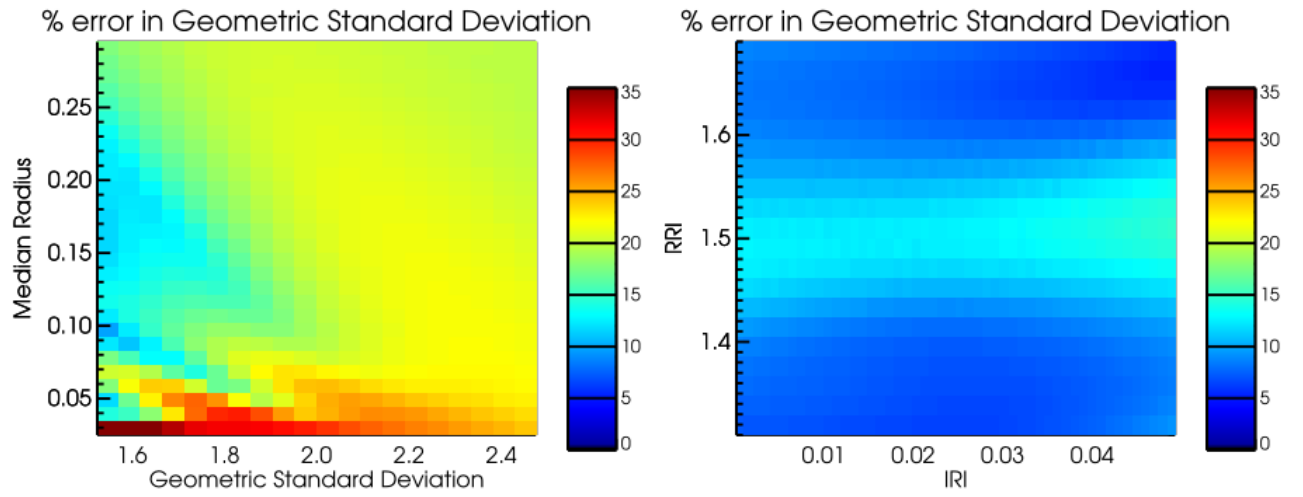

Figure S 2. Like Figure S 1 but for the a posteriori standard deviation in the geometric standard deviation.

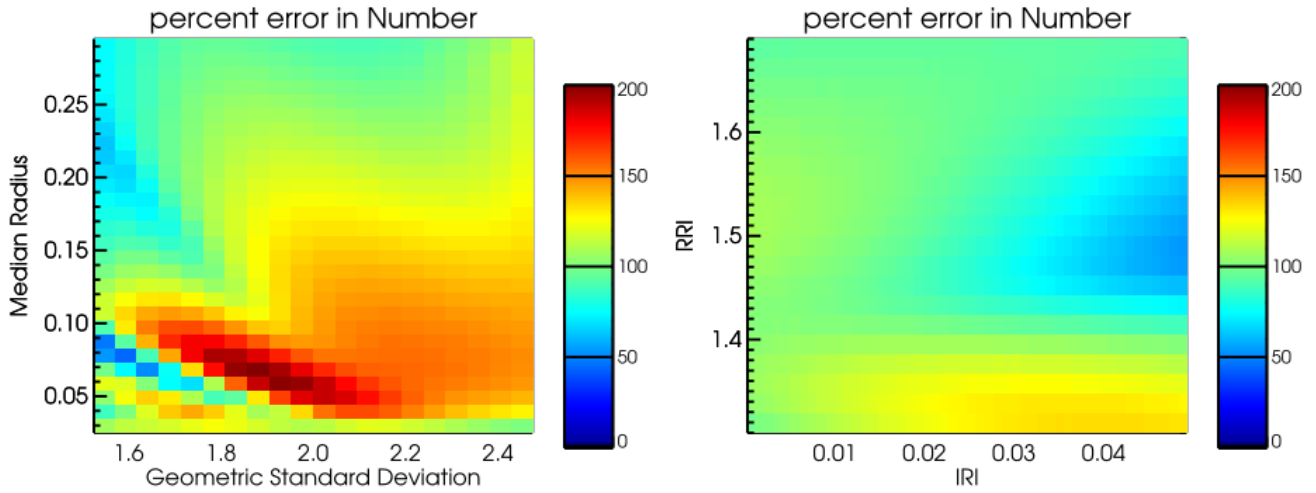

Figure S 3. Like Figure S 1 but for the a posteriori standard deviation in the total number concentration.

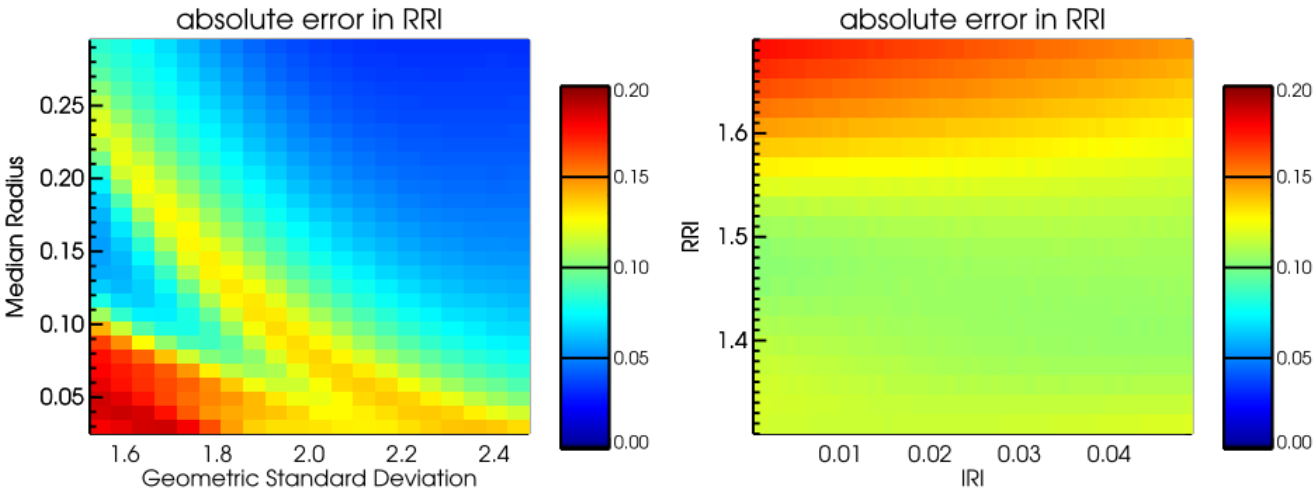

Figure S 4. Like Figure S 1 but the a posteriori standard deviation in the real part of the complex refractive index is here shown as an absolute uncertainty.

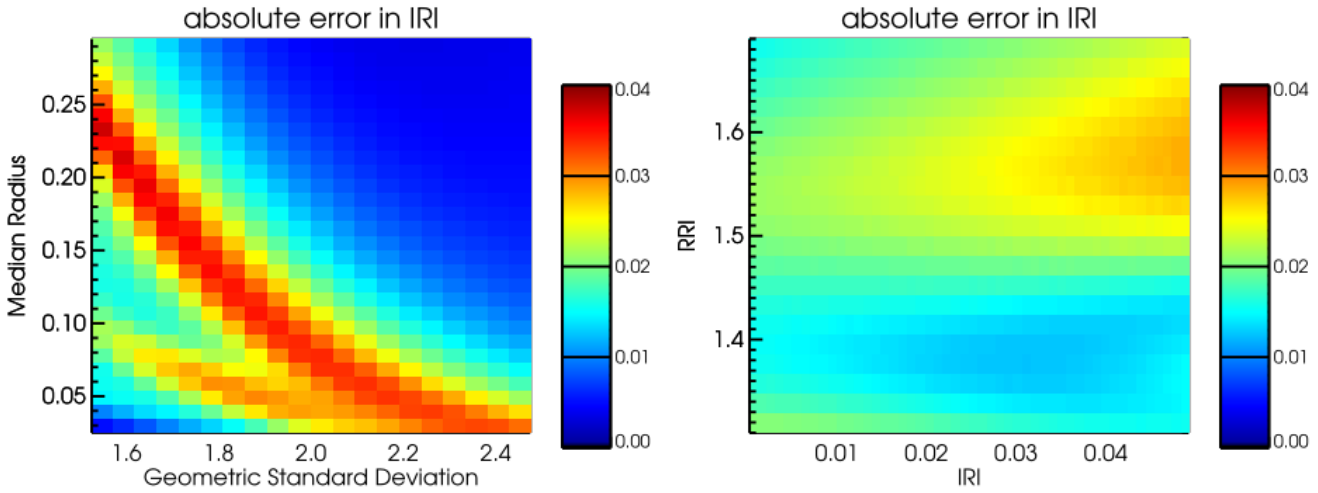

Figure S 5. Like Figure S 4 but for the a posteriori standard deviation in the imaginary part of the complex refractive index.

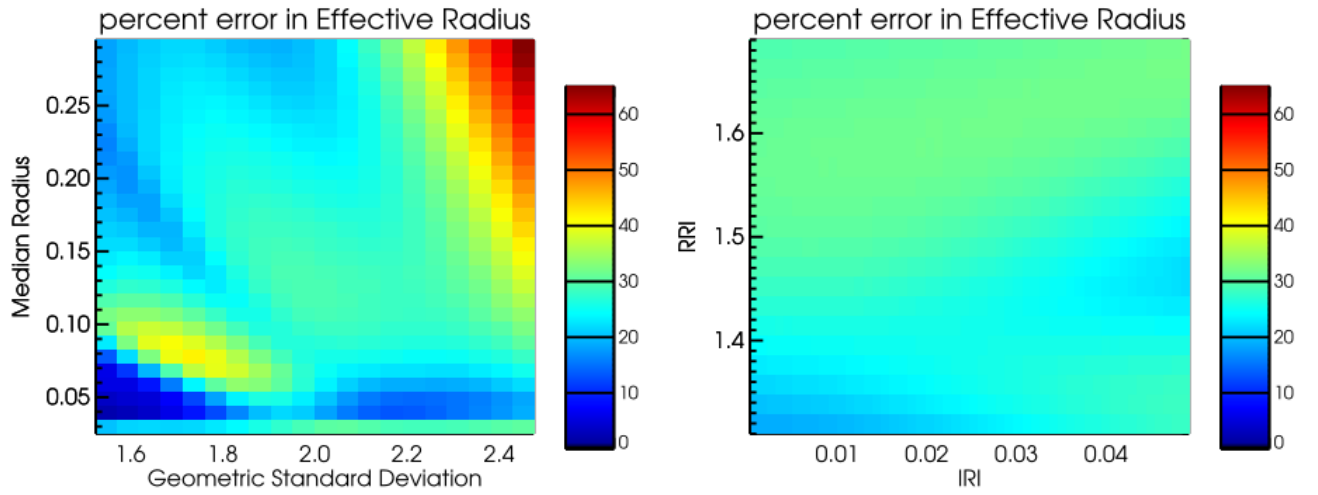

Figure S 6. The derived standard deviation in the effective radius is here shown as a percent error, for the same 2-D slices as Figures S 1-5.

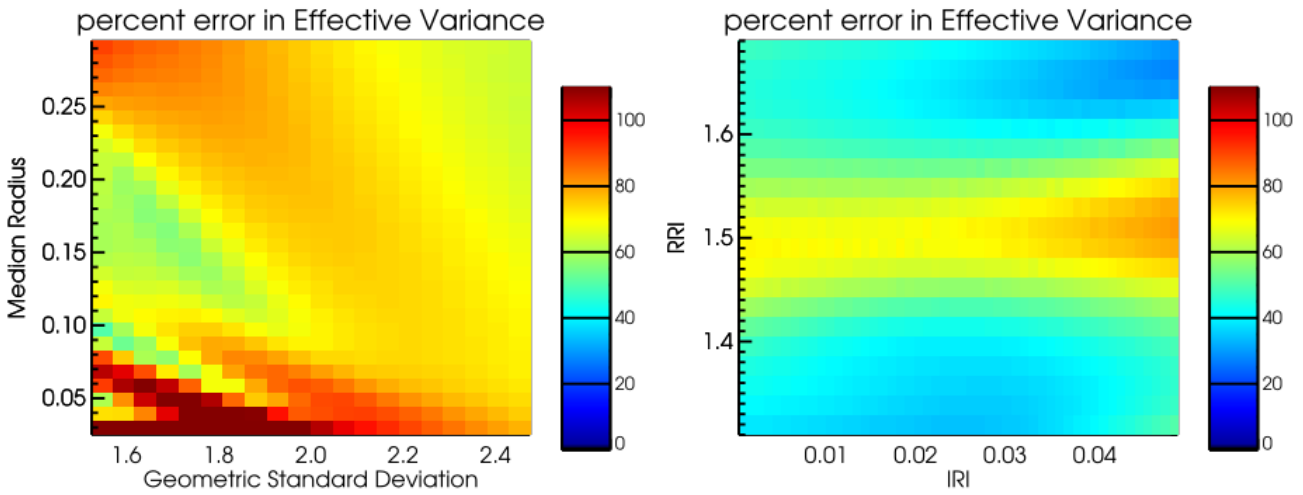

Figure S 7. The derived standard deviation in the effective variance is here shown as a percent error, for the same 2-D slices as Figures S 1-6.

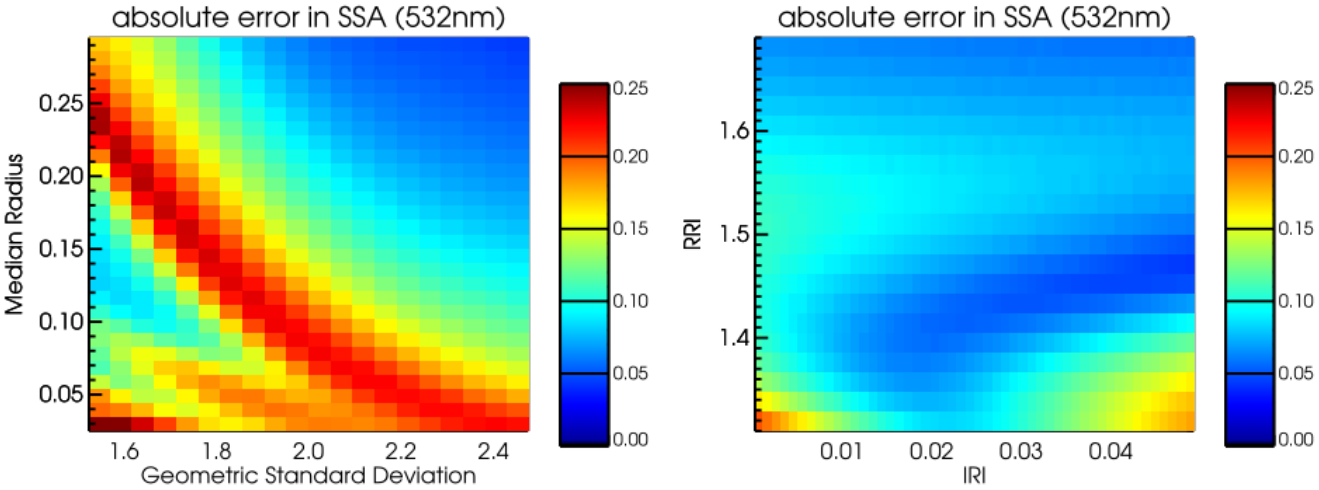

Figure S 8. The derived standard deviation in the single scattering albedo (532 nm) is here shown for the same 2-D slices as Figures S 1-7.

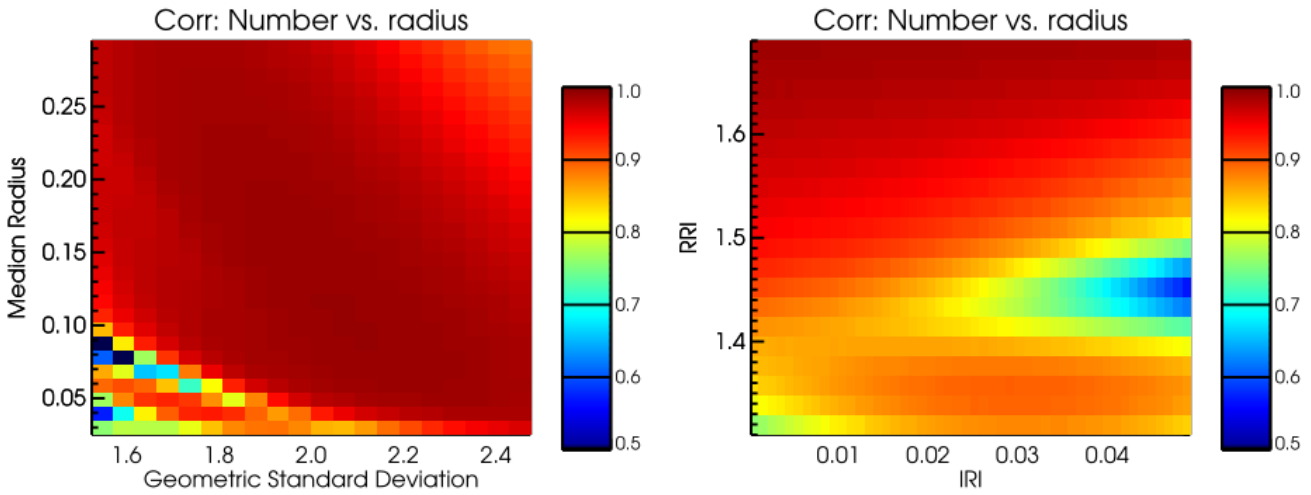

Figure S 9. The a posteriori correlation between retrieved total number concentration and median radius is here shown for the same 2-D slices as Figures A 1-8.

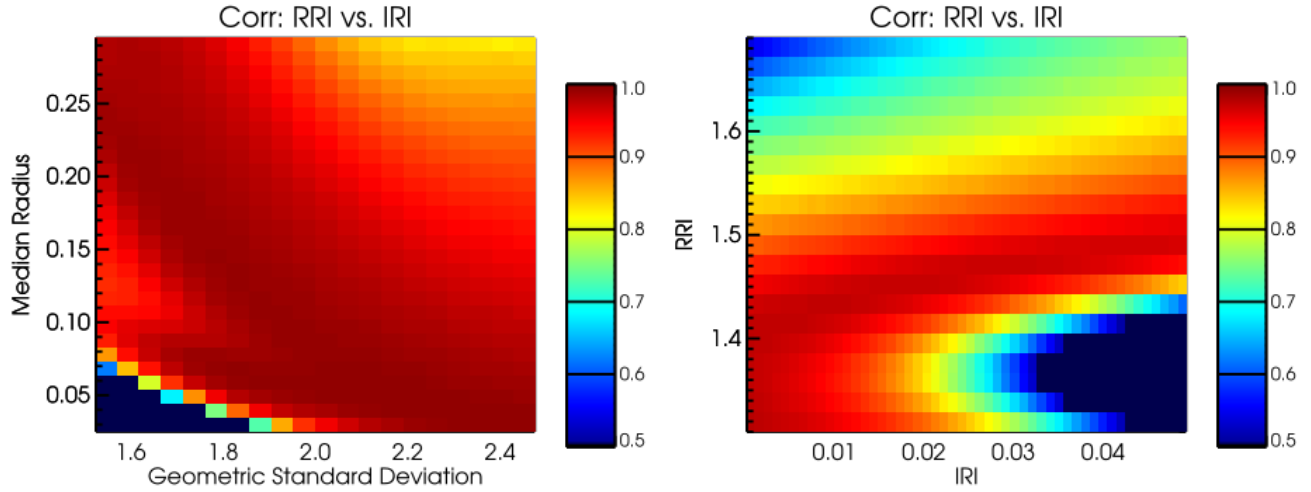

Figure S 10. Like Figure S 9 but for the a posteriori correlation between retrieved real refractive index and imaginary refractive index.